

**21st International Conference on  
Harmonisation within Atmospheric Dispersion Modelling for Regulatory Purposes  
27-30 September 2022, Aveiro, Portugal**

---

**SMOKE PLUME FROM FIRE LAGRANGIAN SIMULATION: DEPENDENCE ON DRAG  
COEFFICIENT AND RESOLUTION**

*Bianca Tenti<sup>1,2</sup>, Enrico Ferrero<sup>1,3</sup>*

<sup>1</sup>Università del Piemonte Orientale, Vercelli, Italy

<sup>2</sup>Università di Torino, Torino, Italy

<sup>3</sup>ISAC-CNR, Torino, Italy

**Abstract:** In this work a numerical simulation of the plume dispersed from a fire is performed using the Lagrangian stochastic particle model SPRAYWEB and the results are compared to a field experiment, carried out in August 2013 in Idaho (USA). The plume rise scheme used is not based on an analytical model and the only two assumptions required are the drag coefficient ( $C_D$ ) value and the cell size. Here we want to assess the dependence of the model on the values chosen for these two parameters.

**Key words:** *Plume rise, dispersion model, drag coefficient*

## INTRODUCTION

Correct modeling of the plume rise is fundamental for a proper description of pollutants dispersion, especially for highly buoyant wildfire plumes. In this work, a numerical simulation of the plume dispersed from a fire is performed applying the recent plume rise scheme suggested by Alessandrini et al. (2013) introduced in the Lagrangian stochastic particle model SPRAYWEB (Tinarelli et al., 2000, Alessandrini and Ferrero, 2009, Ferrero et al., 2022) and the results are compared to ground-based mobile elastic scanning lidar measurements of the maximum height of a plume coming from a prescribed 66 ha burn ignited during a field experiment, carried out in August 2013 in Idaho (USA) (Kovalev et al., 2014, Zhou et al., 2018). According to the algorithm, the plume is split into many cubic grid cells and at each time step the temperature and the momentum difference between the plume and background atmosphere is computed for each cell. One of the greatest advantages of this plume rise scheme is that it is not based on an analytical model and the only two assumptions required are the drag coefficient value and the cell size. With the aim of finding a general expression for the drag coefficient and a rule for the choice of the grid cells dimension, we assess the dependence of the model on the values chosen for these two parameters. So far, given the lack of a generally accepted value in the literature, the drag coefficient proposed by Ooms (1972) was adopted. However, different  $C_D$  expressions can be found in the literature; some of them are here tested comparing model results with experimental datasets.

Furthermore, to improve the results, we also perform some tests to estimate the optimal source-to-cell size ratio for the horizontal grid. The results are presented in terms of the comparison of the maximum plume height trend predicted by the model and the observations. An evaluation of the best model for  $C_D$  is shown through the Taylor diagram.

## THE PLUME RISE SCHEME AND DRAG COEFFICIENT MODELS

The plume rise scheme suggested by Alessandrini et al. (2013) is based on the Lagrangian description of the plume evolution in terms of particle trajectories, while the temperature and momentum differences, which are responsible for the plume buoyancy, are calculated on a fixed grid. At each time step  $\Delta t = t_1 - t_0$  temperature and momentum differences ( $\Delta T$  and  $w_c$  respectively) between each grid cubic cell and the surrounding environment are computed using the following equations:

$$\Delta T(t_1) = \Delta T(t_0) + \Gamma(z_c)w_c(t_0)\Delta t + 0.0098w_c(t_0)\Delta t, \quad (1)$$

$$w_c(t_1) = w_c(t_0) + \frac{\Delta T_c(t_1)}{\Delta T_c + T_a(z_c)} g \Delta t - \frac{0.5 C_D S w_c^2(t_0) \rho_a}{\rho_p V_c} \Delta t, \quad (2)$$

where  $z_c$  is the cell height,  $T_a$  the ambient temperature,  $g$  the gravity,  $C_D$  the drag coefficient,  $S$  and  $V_c$  the cell section and volume,  $\rho_a$  and  $\rho_p$  the ambient and plume density.

Four drag coefficient expressions which depend on the Reynolds number of the cells ( $Re_c$ ) are tested comparing the model results with respect to observations.

For each cell the correspondent Reynolds number is calculated as follows:

$$Re_c = \varphi \frac{|U_c|}{\nu}, \quad (3)$$

where  $\varphi$  is the equivalent cell diameter,  $V_c$  is the cell vertical velocity and  $\nu$  is the kinematic viscosity of air.

**Table 1.** Drag coefficient expressions.

Author	$C_D$ expression	
Turton and Levenspiel (1986)	$C_D = \frac{24}{Re_c} (1 + 0.173 Re_c^{0.657}) + \frac{0.413}{1 + 16300 Re_c^{-1.09}}, \text{ if } Re_c < 2 \times 10^5$	(4)
Brown and Lawler (2003)	$C_D = \frac{24}{Re_c} (1 + 0.15 Re_c^{0.681}) + \frac{0.407}{1 + 8710 Re_c^{-1}}, \text{ if } Re_c < 2 \times 10^5$	(5)
Cheng (2009)	$C_D = \frac{24}{Re_c} (1 + 0.27 Re_c)^{0.43} + 0.47 (1 - \exp(-0.04 Re_c^{0.38}))$	(6)
Mikhailov and Silva Freire (2013)	$C_D = \frac{777 \left( \frac{669806}{875} \right) + \left( \frac{114976}{1155} \right) Re_c + \left( \frac{707}{1380} \right) Re_c^2}{646 Re_c \left( \frac{32869}{952} \right) + \left( \frac{924}{643} \right) Re_c + \left( \frac{1}{385718} \right) Re_c^2}$	(7)

The first three expressions presented in Table 1 are similar, as a sort of Stokes' law extended for higher Reynolds numbers, but with different constants derived by fitting experimental data. The latter is derived from the Shanks transformation of Goldstein series (Goldstein, 1929, Shanks, 1955) improved by fitting its coefficients directly to experimental data. These four expressions are implemented within the plume rise scheme. As meteorological input we use the WRF simulation provided by Ferrero et al. (2019), with turbulence field reconstructed by WSI (WRF-SPRAYWEB Interface). The dispersion is simulated by the Lagrangian Stochastic model SPRAYWEB and the results are compared to measurements taken during the field experiment organized by the US Environmental Protection Agency (EPA) over complex terrain in Idaho with a ground-based mobile elastic scanning lidar (Kovalev et al., 2014, Zhou et al., 2018).

## RESULTS

Figure 1 shows the maximum height of the plume as a function of time predicted by the model compared with the observations. In order to estimate the maximum plume height we consider two vertical standard deviation of the plume distribution above the mean particles height.

Data are smoothed using a moving-average smoothing function; the different colors indicate results obtained using different expressions for the drag coefficient and lidar observations of maximum plume height are also reported (black circles).

Almost all the models well reproduce lidar measurements in the second phase of the simulation, except for the Mikhailov and Silva Freire (2013) one. As for the initial phase of the event, observations are probably not very reliable since the values measured by the lidar are higher than the ones taken during the stability phase of the plume. The discrepancies between the observations and the model results could be due to a very fluctuating behavior of the plume in the initial phase which causes the lidar to measure very high values.

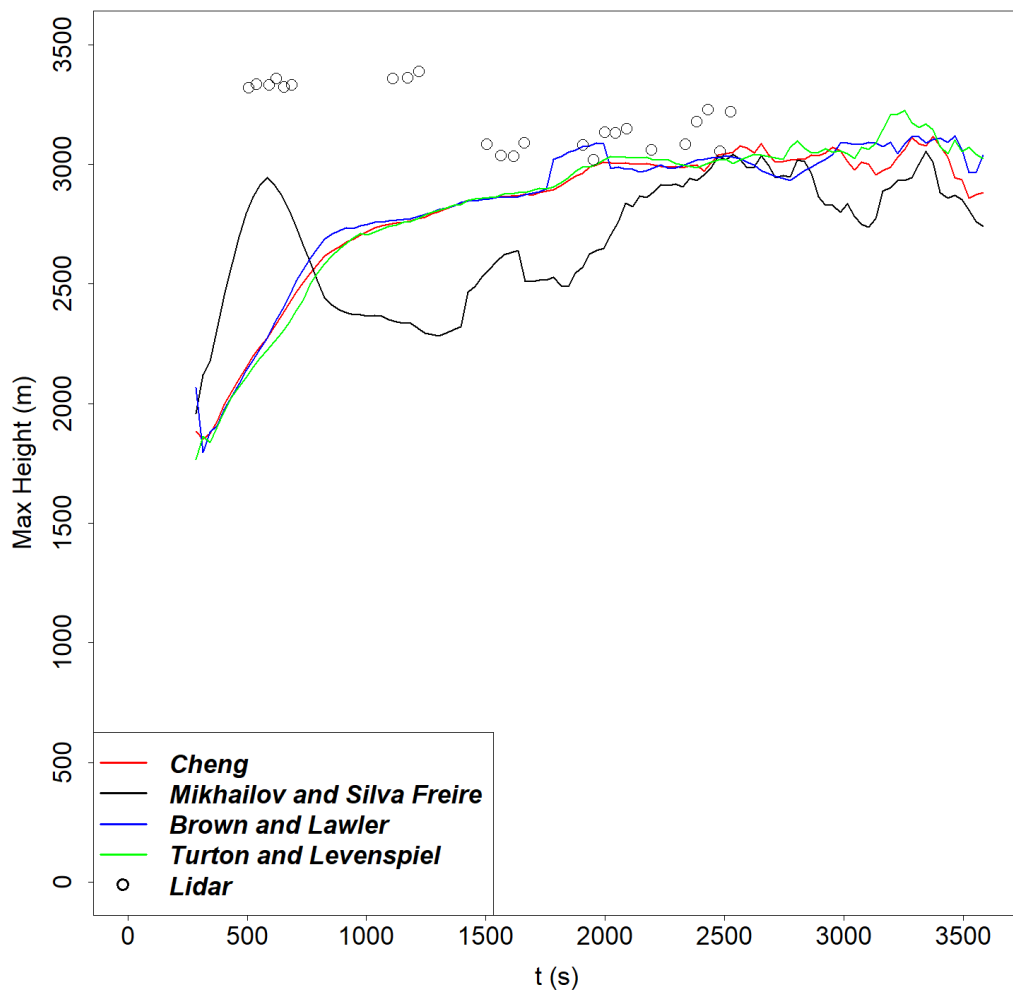


**Figure 1.** Plume maximum height as a function of time

Given the possible low reliability of the data observed during the first phase of the fire, the Taylor diagram presented in Figure 2 is created considering only the stability phase of the plume. In general, this analysis shows that there are differences between the four models which are hardly visible by observing Figure 1. Turton and Levenspiel (1986) model shows a very low correlation, while the correlation of the other models is around 0.4-0.5. As expected Mikhailov and Silva Freire (2013) expression for drag coefficient gives the highest root mean squared error. The two most faithful models are those of Cheng (2009) and Brown and Lawler (2003).

As for the horizontal resolution of the plume rise scheme, we performed some simulations varying the dimension of the grid cells, and we found that there is no particular dependence of the results on it.

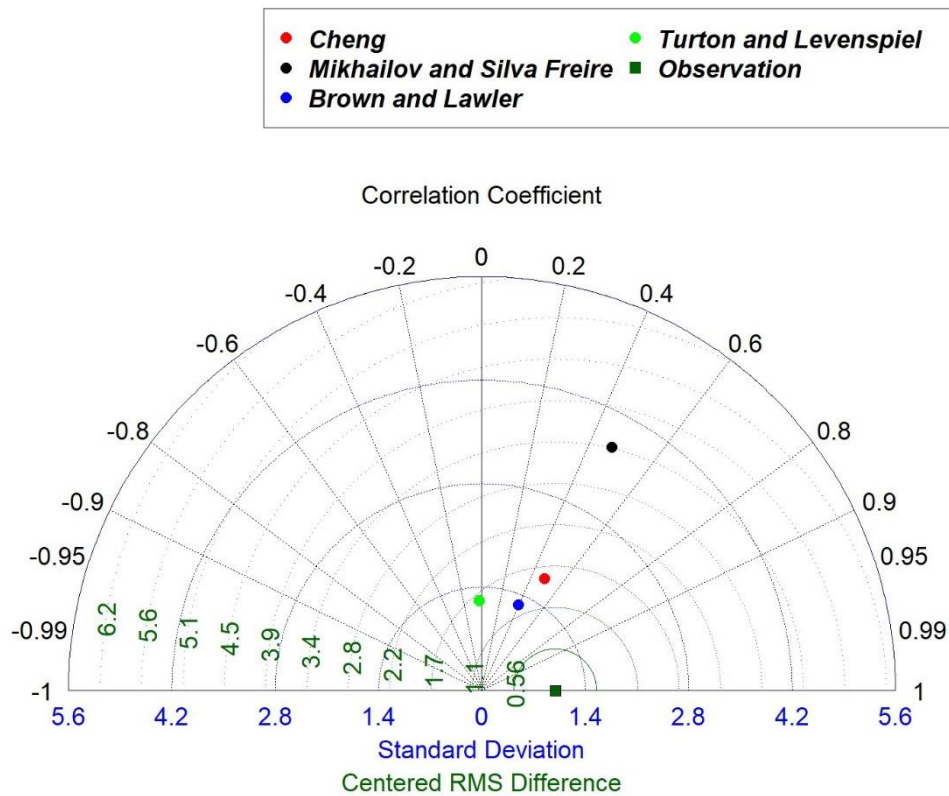


Figure 2. Taylor diagram for the four drag coefficient expressions

## CONCLUSIONS

In this work we studied the dependence of the plume rise scheme embedded in the Lagrangian Stochastic model SPRAYWEB on the drag coefficient and on the horizontal resolution. We tested 4 different expressions of the drag coefficient depending on the Reynolds number found in the literature, three of which are derived from Stokes' law and one from the Shanks transformation of Goldstein series (Goldstein, 1929, Shanks, 1955). Generally speaking, from the results it is evident that for this type of application the models deriving from the Stokes law have a better performance. In particular, the models of Cheng (2009) and Brown and Lawler (2003) give results that better agree with the observations. The model of Cheng (2009) and Brown and Lawler (2003) can only be applied in case of Reynolds numbers less than  $2 \times 10^5$ , while the one of Cheng (2009) has no restrictions and this makes it the best choice for our purposes. Regarding the horizontal resolution we did not find a strong dependence of the results in case of small prescribed fires. As future work we want to test the same drag coefficient expressions on other case studies to confirm what emerged in this study.

## ACKNOWLEDGMENTS

Part of the activities were carried out in the framework of SAPERI Project, funded by Aethia Srl and Regione Piemonte (POR FESR 2014/2020 - Asse I - Azione I.1b.1.2 - Bando PRISM-E).

## REFERENCES

- Alessandrini, S. and E. Ferrero, 2009: A hybrid lagrangian-eulerian particle model for reacting pollutant dispersion in non-homogeneous non-isotropic turbulence. *Physica A*, 388 (8), 1375– 1387.
- Alessandrini, S., Ferrero, E., and Anfossi, D., 2013: A new Lagrangian method for modelling the buoyant plume rise. *Atmospheric environment*, 77, 239-249.
- Brown, P. P., and Lawler, D. F., 2003: Sphere drag and settling velocity revisited. *Journal of environmental engineering*, 129(3), 222-231.

- Cheng, N. S., 2009: Comparison of formulas for drag coefficient and settling velocity of spherical particles. *Powder Technology*, 189(3), 395-398.
- Ferrero, E., Alessandrini, S., Anderson, B., Tomasi, E., Jimenez, P., and Meech, S., 2019: Lagrangian simulation of smoke plume from fire and validation using ground-based lidar and aircraft measurements. *Atmospheric Environment*, 213, 659-674.
- Ferrero, E., Alessandrini, S., Meech, S., and Rozoff, C., 2022: A 3D Lagrangian stochastic particle model for the concentration variance dispersion. *Bull. of Atmos. Sci. & Technol.* **3**, 2.
- Goldstein, S., 1929: The steady flow of viscous fluid past a fixed spherical obstacle at small Reynolds numbers. *Proceedings of the Royal Society of London*, 123(791), 225-235.
- Kovalev, V., Urbanski, S., Petkov, A., Scalise, A., Wold, C., and Hao, W. M., 2014: Validation of smoke plume rise models using ground-based Lidar. In *Remote Sensing for Agriculture, Ecosystems, and Hydrology XVI* (Vol. 9239, pp. 478-486). SPIE.
- Mikhailov, M. D. and Freire, A. S., 2013: The drag coefficient of a sphere: An approximation using Shanks transform. *Powder technology*, 237, 432-435.
- Shanks, D., 1955: Non-linear transformations of divergent and slowly convergent sequences. *Journal of Mathematics and Physics*, 34(1-4), 1-42.
- Tinarelli, G., Anfossi, D., Trini Castelli, S., Bider, M., Ferrero, E., 2000: A New High Performance Version of the Lagrangian Particle Dispersion Model Spray, Some Case Studies. *Springer US*, Boston, MA, pp. 499–507.
- Turton, R. and Levenspiel, O., 1986: A short note on the drag correlation for spheres. *Powder technology*, 47(1), 83-86.
- Zhou, L., Baker, K. R., Napelenok, S. L., Pouliot, G., Elleman, R., O'Neill, S. M., Urbanski, S. P., and Wong, D. C., 2018: Modeling crop residue burning experiments to evaluate smoke emissions and plume transport. *Science of The Total Environment*, 627, 523-533.